State preparation of a fluxonium qubit with feedback from a custom FPGA-based platform

Richard Gebauer,^{1,*} Nick Karcher,¹ Daria Gusenkova,² Martin Spiecker,² Lukas Grünhaupt,² Ivan Takmakov,^{2,3,4} Patrick Winkel,² Luca Planat,⁵ Nicolas Roch,⁵ Wolfgang Wernsdorfer,^{2,3,5} Alexey V. Ustinov,^{2,4} Marc Weber,¹ Martin Weides,^{2,6} Ioan M. Pop,^{2,3} and Oliver Sander¹

¹Institute for Data Processing and Electronics, Karlsruhe Institute of Technology, 76131 Karlsruhe, Germany
²Physikalisches Institut, Karlsruhe Institute of Technology, 76131 Karlsruhe, Germany
³Institute of Nanotechnology, Karlsruhe Institute of Technology, 76344 Eggenstein-Leopoldshafen, Germany
⁴Russian Quantum Center, National University of Science and Technology MISIS, Moscow 119049, Russia
⁵Université Grenoble Alpes, CNRS, Grenoble INP, Institut Néel, 38000 Grenoble, France
⁶James Watt School of Engineering, University of Glasgow, Glasgow G12 8LT, United Kingdom
(Dated: January 15, 2022)

We developed a versatile integrated control and readout instrument for experiments with superconducting quantum bits (qubits), based on a field-programmable gate array (FPGA) platform. Using this platform, we perform measurement-based, closed-loop feedback operations with 428 ns platform latency. The feedback capability is instrumental in realizing active reset initialization of the qubit into the ground state in a time much shorter than its energy relaxation time T_1 . We show experimental results demonstrating reset of a fluxonium qubit with 99.4% fidelity, using a readout-and-drive pulse sequence approximately 1.5 μ s long. Compared to passive ground state initialization through thermalization, with the time constant given by $T_1 = 80 \,\mu$ s, the use of the FPGA-based platform allows us to improve both the fidelity and the time of the qubit initialization by an order of magnitude.

The control of superconducting quantum bits (qubits) [1–5] relies on the ability to read out their state with high precision and apply custom pulses, conditioned on the result of the readout, on a time scale much shorter than the qubit lifetime T_1 . For the same signal integration time, the readout fidelity can be increased significantly using Josephson parametric amplifiers (JPAs) [6–9]. The rapid signal processing and decision taking, on the other hand, requires custom hardware based on field-programmable gate arrays (FPGAs), as recently demonstrated in Refs. [10–12].

Here we present a versatile FPGA-based control and readout platform for experiments with superconducting qubits, which enables fast (compared to T_1) feedback loops to control qubits depending on their state. This type of dynamical and conditional control sequences provides the basis for experiments and algorithms relevant for quantum computation, such as active reset [10] or quantum error correction [12].

To perform such closed loops, we employ measurement-based feedback where the qubit, dispersively coupled to a readout resonator [13, 14], is first projected by an initial quantum non-demolition measurement [15–17] onto its ground or excited state, $|0\rangle$ or $|1\rangle$, respectively. The result of this measurement is evaluated in real-time on our platform, by separating the plane of the in-phase and quadrature (IQ) components of the readout resonator response signal in two semiplanes, one attributing the measurement outcome to state $|0\rangle$, the other to state $|1\rangle$. This is achieved by performing linear discriminant analysis which, in case of symmetric and state-independent noise on the response signal, represents also the optimal Bayesian classifier [18]. Based on the result, different pulse sequences can follow to further manipulate the qubit.

An important figure of merit is the response time or feedback latency of the platform. In the current state of development we report a platform latency of 428 ns. This starts to be advantageous in state preparation protocols for typical superconducting qubits, with energy relaxation times T_1 exceeding tens of microseconds. The response time is defined as the delay between the last sample of the readout pulse entering the platform and the first sample of the output pulse, which is conditioned on the acquired information. It is platform-specific and therefore does not include experimental parameters such as the propagation delay through the microwave lines connecting to the cryogenic setup, or the duration of the readout pulse. The response time is solely determined by internal delays of the electronics. The main contributions are given by the conversion from the analog to the digital domain and back, as well as by decimation and interpolation filters used to reduce the sample rate in the digital domain. We estimate that latencies as low as 150 ns are possible with an optimized platform design.

Currently, the platform consists of a Xilinx Zynq UltraScale+ RFSoC ZCU111 Evaluation Board with a XCZU28DR-2FFVG1517E chip. It integrates the FPGA, two processors, eight 6.554 GSPS 14 bit digital-to-analog and eight 4.096 GSPS 12 bit analog-to-digital converters. Our FPGA firmware runs at a clock speed of 125 MHz and handles signals at a sample rate of 500 MSPS. Input and output signals are decimated and interpolated from and to 4 GSPS, which is the sample rate at which the converters operate. The platform has four output channels, designed to operate as two IQ pairs, one intended for qubit manipulation pulses and one for the readout. The platform further provides two input channels to acquire the readout pulses which passed through the experimental setup. Here, we use them to digitize the signal and reference from an interferometer setup (see experimental

^{*} Corresponding author: richard.gebauer@kit.edu

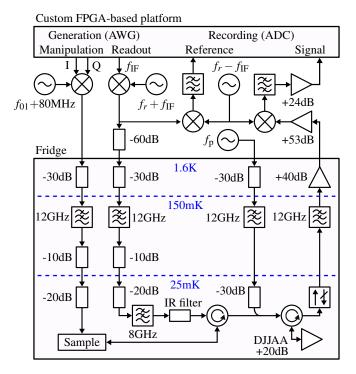


FIG. 1. Interferometer setup with custom FPGA-based platform for time-domain experiments. The platform offers two IQ channels to generate shaped pulses for the readout and manipulation of the sample. In this setup, only one quadrature of the readout pulse is used. The frequencies of the pulses are $f_{\rm IF} = 62.5\,{\rm MHz}$ and $80\,{\rm MHz}$, respectively. By using a single side-band mixer for the readout and an IQ mixer for the manipulation pulse, the microwave signals are upconverted to the desired resonator and qubit frequencies $f_{\rm r}$ and f_{01} , respectively. The readout pulse is split before the cryostat input. One branch is directly downconverted and used as reference by the platform. The other branch of the signal is routed through the cryogenic measurement setup, after which it is amplified, downconverted and digitized at the signal input of the platform. From the evaluation of these two signals on the platform we obtain the I and Q components.

schematics in Fig. 1). In our case, single side-band mixers are employed and the readout pulse is split after upconversion. One branch is directly downconverted and serves as the reference signal. The other branch passes through the cryostat and is modulated by the sample before being downconverted as well.

After digitization, the FPGA first compensates the different cable delays by delaying the reference signal, according to an initial calibration. It then extracts the I and Q components by interfering the signal with the analytic representation [19] of the reference. This is achieved by multiplying the signal point-wise with the reference resulting in a value for the I component. In a separate multiplication to obtain the Q component, the reference is first shifted by $\pi/2$. For intermediate frequencies close to $f_{\rm IF}=62.5\,{\rm MHz}$, this corresponds to a shift of two samples on the FPGA. Afterwards the two products are summed up for a recording time of 800 ns corresponding to the duration of the readout pulse. The obtained values for the I and Q components of the signal are then evaluated in order to infer the state of the qubit. Acquisition, IQ calcula-

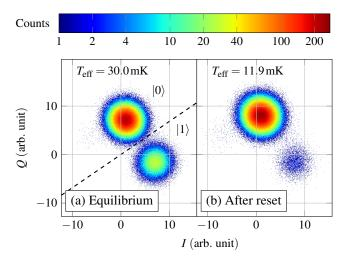


FIG. 2. Demonstration of quantum feedback by using an active reset sequence. (a) shows the cavity response before the active reset operation while the qubit is in thermal equilibrium with the environment. The linear discriminant used to determine the qubit state in real-time on our platform is indicated as dashed line. (b) shows the response directly after preparing the qubit in its ground state $|0\rangle$ with an active reset operation.

tion, as well as qubit state estimation can run continuously, in parallel and in a pipelined manner. By offering the possibility to continue with a different pulse sequence after each qubit state estimation, the platform allows the user to react to this state in real-time. For example, one of the most basic protocols employing this capability is to initialize the state of the qubit on the fly.

Indeed, high-fidelity and rapid state initialization become an essential prerequisite for almost any experimental sequence as the coherence properties of superconducting qubits improve [20–26]. Generally speaking one can opt to perform either an autonomous stabilization sequence [27, 28], or to use active reset to initialize the qubit state within a few microseconds, significantly faster than the thermalization time.

To test the feedback capabilities of our platform, we perform active reset on a superconducting granular aluminum fluxonium qubit [21] dispersively coupled to a readout cavity. We start by measuring the qubit state with relatively long readout pulses of 800 ns, boosted by a dispersion engineered Josephson junction array parametric amplifier (DJJAA) [8]. The state is encoded in the amplitude and phase of the cavity response signal due to the dispersive frequency shift [13, 14] of the cavity. From this information (which is represented in the IQ-plane) the qubit state is estimated. If the platform detects the excited state $|1\rangle$, a π pulse is executed to rotate it to the ground state $|0\rangle$. If state $|0\rangle$ is recognized, no π pulse follows. Thereby, after the operation, the qubit is prepared in its ground state.

We report reset fidelities up to 99.4 %. The fidelity is determined by first letting the qubit thermalize and then performing the active reset operation followed by an additional readout to characterize the resulting state. The probability to end up in the ground state $|0\rangle$ after the reset is equivalent to the

fidelity of the active reset operation. Histograms of the response in the IQ-plane of the cavity coupled to the fluxonium qubit, before and after the active reset operation, are shown in Fig. 2. Each histogram comprises one million single-shot measurements and was directly obtained by the platform. The dispersive frequency shift of the cavity makes the two states distinguishable and allows us to directly extract the qubit state population from the histograms.

In thermal equilibrium, right before the operation, a $|1\rangle$ state population of 11.7% is obtained. Considering the transition frequency $f_{01}=1.26\,\mathrm{GHz}$ of the fluxonium qubit at the flux and T_1 sweet spot [26], this population corresponds to an effective temperature of 30.0 mK, comparable to the temperature of the cryostat mixing chamber. Directly after the reset operation, the $|1\rangle$ state population is only 0.6%. We thereby achieved an effective cooling of the qubit to 11.9 mK. The achieved reset fidelity is limited by the experimental setup and choice of parameters, setting the state discrimination in the IQ-plane. The Bayesian error alone places an upper bound of 99.5% fidelity.

To summarize, our FPGA-based platform enables qubit ground state initialization with 99.4% fidelity, using a sequence approximately $1.5\,\mu s$ long, out of which only 428 ns account for the intrinsic platform latency. Future efforts will focus on reducing this platform latency down to 150 ns, and operating at larger readout powers, which should increase the

qubit state separation and decrease the readout pulse duration below 100 ns [29].

ACKNOWLEDGMENTS

Funding was provided by the Initiative and Networking Fund of the Helmholtz Association, within the Helmholtz Future Project 'Scalable solid state quantum computing' and the Alexander von Humboldt Foundation in the framework of a Sofja Kovalevskaja award endowed by the German Federal Ministry of Education and Research. R. Gebauer acknowledges support by the Helmholtz International Research School for Teratronics (HIRST). N. Karcher acknowledges support by the Karlsruhe School of Elementary Particle and Astroparticle Physics (KSETA). I. Takmakov and A.V. Ustinov acknowledge support from the Ministry of Education and Science of the Russian Federation in the framework of the Increase Competitiveness Program of the National University of Science and Technology MISIS (contract no. K2-2017-081). M. Weides acknowledges support by the European Research Council (ERC) under the Grant Agreement No. 648011, and the Deutsche Forschungsgemeinschaft (DFG) projects INST 121384/138-1FUGG. Facilities use was supported by the KIT Nanostructure Service Laboratory. We acknowledge Qkit [30] for providing a convenient measurement software framework.

- [1] J. Koch, T. M. Yu, J. Gambetta, A. A. Houck, D. I. Schuster, J. Majer, A. Blais, M. H. Devoret, S. M. Girvin, and R. J. Schoelkopf, Phys. Rev. A 76, 042319 (2007).
- [2] V. E. Manucharyan, J. Koch, L. I. Glazman, and M. H. Devoret, Science 326, 113 (2009).
- [3] M. H. Devoret and R. J. Schoelkopf, Science 339, 1169 (2013).
- [4] P. Krantz, M. Kjaergaard, F. Yan, T. P. Orlando, S. Gustavsson, and W. D. Oliver, Applied Physics Reviews 6, 021318 (2019).
- [5] X. Gu, A. F. Kockum, A. Miranowicz, Y. xi Liu, and F. Nori, Physics Reports 718-719, 1 (2017).
- [6] R. Vijay, D. H. Slichter, and I. Siddiqi, Phys. Rev. Lett. 106, 110502 (2011).
- [7] M. Castellanos-Beltran, K. Irwin, G. Hilton, L. Vale, and K. Lehnert, Nature Physics 4, 929 (2008).
- [8] P. Winkel, I. Takmakov, D. Rieger, L. Planat, W. Hasch-Guichard, L. Grünhaupt, N. Maleeva, F. Foroughi, F. Henriques, K. Borisov, J. Ferrero, A. V. Ustinov, W. Wernsdorfer, N. Roch, and I. M. Pop, arXiv e-prints, arXiv:1909.08037 (2019), arXiv:1909.08037 [quant-ph].
- [9] A. Roy and M. Devoret, Comptes Rendus Physique 17, 740 (2016).
- [10] D. Ristè, C. C. Bultink, K. W. Lehnert, and L. DiCarlo, Phys. Rev. Lett. 109, 240502 (2012).
- [11] P. Campagne-Ibarcq, E. Flurin, N. Roch, D. Darson, P. Morfin, M. Mirrahimi, M. H. Devoret, F. Mallet, and B. Huard, Phys. Rev. X 3, 021008 (2013).
- [12] N. Ofek, A. Petrenko, R. Heeres, P. Reinhold, Z. Leghtas, B. Vlastakis, Y. Liu, L. Frunzio, S. M. Girvin, L. Jiang, M. Mirrahimi, M. H. Devoret, and R. J. Schoelkopf, Nature 536, 441 (2016).
- [13] A. Blais, R. Huang, A. Wallraff, S. M. Girvin, and R. J.

- Schoelkopf, Phys. Rev. A 69, 062320 (2004).
- [14] W. C. Smith, A. Kou, U. Vool, I. M. Pop, L. Frunzio, R. J. Schoelkopf, and M. H. Devoret, Phys. Rev. B 94, 144507 (2016).
- [15] V. B. Braginsky, Y. I. Vorontsov, and K. S. Thorne, Science 209, 547 (1980).
- [16] A. Lupaşcu, S. Saito, T. Picot, P. C. De Groot, C. J. P. M. Harmans, and J. E. Mooij, Nature Physics 3, 119 (2007).
- [17] A. Kou, W. C. Smith, U. Vool, I. M. Pop, K. M. Sliwa, M. Hatridge, L. Frunzio, and M. H. Devoret, Phys. Rev. Applied 9, 064022 (2018).
- [18] J. Beyerer, Pattern recognition: introduction, features, classifiers and principles, edited by M. Richter and M. Nagel, De Gruyter graduate (De Gruyter, Berlin, 2018).
- [19] J. O. Smith, Mathematics of the discrete Fourier transform (DFT): with audio applications (Julius Smith, 2007).
- [20] N. Earnest, S. Chakram, Y. Lu, N. Irons, R. K. Naik, N. Leung, L. Ocola, D. A. Czaplewski, B. Baker, J. Lawrence, J. Koch, and D. I. Schuster, Phys. Rev. Lett. 120, 150504 (2018).
- [21] L. Grünhaupt, M. Spiecker, D. Gusenkova, N. Maleeva, S. T. Skacel, I. Takmakov, F. Valenti, P. Winkel, H. Rotzinger, W. Wernsdorfer, A. V. Ustinov, and I. M. Pop, Nature Materials, 1 (2019).
- [22] R. Barends, J. Kelly, A. Megrant, D. Sank, E. Jeffrey, Y. Chen, Y. Yin, B. Chiaro, J. Mutus, C. Neill, P. O'Malley, P. Roushan, J. Wenner, T. C. White, A. N. Cleland, and J. M. Martinis, Phys. Rev. Lett. 111, 080502 (2013).
- [23] Y.-H. Lin, L. B. Nguyen, N. Grabon, J. San Miguel, N. Pankratova, and V. E. Manucharyan, Phys. Rev. Lett. 120, 150503 (2018).
- [24] H. Paik, D. I. Schuster, L. S. Bishop, G. Kirchmair, G. Catelani,

- A. P. Sears, B. R. Johnson, M. J. Reagor, L. Frunzio, L. I. Glazman, S. M. Girvin, M. H. Devoret, and R. J. Schoelkopf, *Phys. Rev. Lett.* **107**, 240501 (2011).
- [25] Z. K. Minev, K. Serniak, I. M. Pop, Z. Leghtas, K. Sliwa, M. Hatridge, L. Frunzio, R. J. Schoelkopf, and M. H. Devoret, Phys. Rev. Applied 5, 044021 (2016).
- [26] I. M. Pop, K. Geerlings, G. Catelani, R. J. Schoelkopf, L. I. Glazman, and M. H. Devoret, Nature 508, 369 EP (2014).
- [27] K. Geerlings, Z. Leghtas, I. M. Pop, S. Shankar, L. Frunzio, R. J. Schoelkopf, M. Mirrahimi, and M. H. Devoret, Phys. Rev. Lett. 110, 120501 (2013).
- [28] K. W. Murch, U. Vool, D. Zhou, S. J. Weber, S. M. Girvin, and I. Siddiqi, Phys. Rev. Lett. 109, 183602 (2012).
- [29] J. Heinsoo, C. K. Andersen, A. Remm, S. Krinner, T. Walter, Y. Salathé, S. Gasparinetti, J.-C. Besse, A. Potočnik, A. Wallraff, and C. Eichler, Phys. Rev. Applied 10, 034040 (2018).
- [30] https://github.com/qkitgroup/qkit.